Site-Specific 1,N^6-Ethenoadenylated Single-Stranded Oligonucleotides as Structural Probes for the T4 Gene 32 Protein–ssDNA Complex†

David P. Giedroc,* Raza Khan, and Keith Barnhart
Department of Biochemistry and Biophysics, Texas A&M University, College Station, Texas 77843-2128
Received December 27, 1990; Revised Manuscript Received May 24, 1991

ABSTRACT: Bacteriophage T4 gene 32 protein (g32P) is a DNA replication accessory protein that binds single-stranded (ss) nucleic acids nonspecifically, independent of nucleotide sequence. G32P contains 1 mol of Zn(II)/mol of protein monomer, which can be substituted with Co(II), with maintenance of the structure and activity of the molecule. The Co(II) is coordinated via approximately tetrahedral ligand symmetry by three Cys sulfur atoms and therefore exhibits intense $S^- \rightarrow$ Co(II) ligand to metal charge-transfer (LMCT) transitions in the near ultraviolet [Giedroc, D. P., et al. (1986) *Proc. Natl. Acad. Sci. U.S.A. 83*, 8452–8456]. A series of fluorescent 1,N^6-ethenoadenosine (ϵA)-containing oligonucleotides conforming to the structure (5′ → 3′) d[$(Tp)_m\epsilon A(pT)_{l-m-1}$] where $0 \leq m \leq l - 1$ and length (l) six or eight nucleotides have been evaluated as dynamics probes and potential fluorescence energy transfer donors to Co(II) in mapping the spatial proximity of the (fixed) intrinsic metal ion and a variably positioned ϵA-base in a series of protein–nucleic acid complexes. We provide spectroscopic evidence that the ϵA-oligonucleotides bind to g32P-(A+B) with a *fixed polarity* of the phosphodiester chain. A Trp side chain(s) makes close approach to a ϵA base positioned toward the 3′ end of a bound $l = 8$ oligonucleotide. Six oligonucleotides of $l = 8$ and $m = 0$, 1, 3, 5, 6, or 7 were investigated as energy transfer donors to Co(II) at 0.1 M NaCl, pH 8.1, 25 °C upon binding to Co(II)-substituted or Zn(II) g32P-(A+B), i.e., in the presence and absence of an energy acceptor, respectively. Detectable quenching of the ϵA-fluorescence by the Co(II)-LMCT acceptors was found to occur in all ϵA-oligonucleotide–protein complexes, yielding energy transfer efficiencies (E) of 0.43, 0.31, 0.26, 0.26, 0.28, and 0.41 for $l = 8$ and $m = 0$, 1, 3, 5, 6, and 7 ϵA-oligonucleotides, respectively. The two-dimensional distances R (in Å) were found to vary as follows: d[$\epsilon A(pT)_7$] ($m = 0$), 16.0 (15.5–16.9); d[$Tp\epsilon A(pT)_6$] ($m = 1$), 17.7 (16.9–19.1); d[$(Tp)_3\epsilon A(pT)_4$] ($m = 3$), 20.7 (19.5–22.1); d[$(Tp)_5\epsilon A(pT)_2$] ($m = 5$), 20.5 (19.5–21.9); d[$(Tp)_6\epsilon$ApT] ($m = 6$), 19.0 (18.0–20.4); and d[$(Tp)_7\epsilon$A] ($m = 7$), 18.6 (17.8–19.8). In the context of the estimated dimensions of the g32P-A monomer (25 × 25 × 65 Å), these distances place the metal ion proximate to the bound ssDNA ligand. They further suggest a relatively *closer* approach of the Co(II) to the *both* the 5′ and 3′ nucleotide bases with the internal bases becoming farther removed from the Co(II) toward the middle of the $l = 8$ single strand. These distances are compatible with only a slight helical twist in the phosphodiester backbone of about one-third to one-half turn over the course of the entire octanucleotide when complexed to the core fragment. The structural implications of these findings are discussed.

Gene 32 protein (g32P),[1] encoded by *gene 32* of bacteriophage T4, is a single-stranded (ss) nucleic acid binding protein that binds to regions of ssDNA formed transiently during replication, recombination, and repair processes (Kowalczykowski et al., 1981a; Chase & Williams, 1986; Karpel, 1990). G32P (301 amino acids, M_r 33 487) is a multidomain protein of known primary (Williams et al., 1981) and undefined tertiary structure. Three functional domains become apparent from limited trypsinolysis studies (Moise & Hosoda, 1976; Williams & Konigsberg, 1978). The C-terminal "A" domain (residues 254–301) makes heterologous contacts with other proteins in an active replication complex, including the DNA polymerase and accessory proteins associated with both leading strand and lagging strand DNA synthesis (Burke et al., 1980; Formosa et al., 1983). Tryptic cleavage of this domain from g32P to form g32P-A also removes a kinetic block in the ability of g32P to destabilize natural double-stranded DNAs; equilibrium (thermodynamic) binding parameters remain relatively unchanged (Greve et al., 1978). The N-terminal basic or "B" domain (residues 1–21) is required for g32P to bind with high cooperativity (Spicer et al., 1979). The A and B domains are thought to undergo coupled conformational transitions (Giedroc et al., 1990) to enable high affinity and highly cooperative binding to ssDNA; most if not all protein–nucleic acid contacts are localized in the central trypsin-resistant DNA-binding core domain of the molecule (Karpel, 1990). When liberated from the two terminal domains via limited proteolysis, the central domain is termed the core fragment or g32P-(A+B) (residues 22–253).[1] g32P-(A+B) coordinates an intrinsic Zn(II) ion, which spectroscopic studies indicate is coordinated by the side-chain S^- atoms of three Cys (residues 77, 87, and 90) and a fourth non-sulfur liganding donor atom, proposed to be His^{81} (Giedroc et al., 1986, 1989; Pan et al., 1989a). The Zn(II) ion provides structural stabilization to the core domain of the molecule, as shown by the reduced

†This work was supported by the Texas Agricultural Experiment Station and Biomedical Research Support Group funds awarded to the College of Agriculture. D.P.G. is the recipient of American Cancer Society Junior Faculty Research Award JFRA-270.
*To whom correspondence should be addressed.

[1] Abbreviations: g32P, gene 32 protein, 301 amino acids; the N-terminal "B" domain, residues 1–21; the C-terminal "A" domain residues 254–301; g32P-(A+B), gene 32 protein lacking both the "A" and "B" domains, also referred to as g32P DNA-binding core fragment and g32P*III; SDS–PAGE, sodium dodecyl sulfate–polyacrylamide gel electrophoresis; HPLC, high-pressure liquid chromatography; Tris, tris(hydroxymethyl)aminomethane; Na_3EDTA, trisodium ethylenediaminetetraacetic acid.

0006-2960/91/0430-8230$02.50/0

thermal stability (Keating et al., 1988) and greatly enhanced susceptibility of the core domain to proteolysis (Giedroc et al., 1986, 1987).

The complex formed between the g32P-(A+B) core fragment and oligonucleotides has proven to be an excellent model for investigating structural details of large cooperatively bound g32P–polynucleotide complex at high resolution, notably by ^{1}H NMR (Prigodich et al., 1984, 1986; Pan et al., 1989b). The focus of these studies has been the identification of specific side chains involved in ssDNA binding. Selective deuteriation techniques have been utilized to reduce the ^{1}H NMR spectral complexity and have permitted detailed investigations of cooperative binding by intact g32P (Pan et al., 1989b). These studies further confirm that the core fragment contains the major determinants that directly interact with the ssDNA, while the terminal domains modulate the binding free energy through other indirect means. ^{1}H NMR, site-directed mutagenesis, and other physicochemical approaches have generally implicated the involvement of several as yet unassigned aromatic side chains, including two tyrosines, two phenylalanines, and at least one tryptophan, as strongly interacting with one or more bases of the bound nucleic acid (Casas-Finet et al., 1988; Shamoo et al., 1989; Pan et al., 1989b).

An important structural detail currently undefined relates to the physical proximity of the intrinsic metal ion within the core domain of g32P and bound nucleic acid ligand. Removal of the metal ion has a significant effect on the stability of the protein–nucleic acid complex, which appears more pronounced in the cooperative binding conformation rather than in the interaction with single-site-sized oligonucleotide ligands (Giedroc et al., 1987; Nadler et al., 1990). Since it is clear that the metal coordination chelate does not increase its coordination number or undergo ligand exchange upon binding ssDNA (Giedroc et al., 1989), the metal ion domain must impart structural stability to the complex by maintaining the high-affinity binding conformation of the protein. How this is accomplished requires elucidation of quantitative details on the role of the Zn(II) in nucleic acid recognition by g32P (Nadler et al., 1990), including definition of the spatial proximity of the intrinsic metal ion and the bound oligonucleotide.

In this report, we determine a set of two-dimensional metal–nucleotide base distances using fluorescence resonance energy transfer (FRET) spectroscopy. Our experimental strategy is to incorporate into a single-stranded oligonucleotide a uniquely positioned nonperturbing fluorescent probe, whose fluorescence emission spectrum would overlap the absorption spectrum of the Co(II) coordination complex in g32P, substituted for the intrinsic Zn(II). We first evaluate the utility of a single 1,N^6-ethenoadenine (ϵA)[2] nucleotide base (Secrist et al., 1972) uniquely positioned in the primary structure of an otherwise unlabeled oligonucleotide to function as a site-specific reporter group in the oligonucleotide–Zn(II) g32P-(A+B) complex (i.e., in the absence of energy acceptor). The ribohomopolymer poly(1,N^6-ethenoadenylic) acid has already proven useful in defining the thermodynamics and structural changes that accompany cooperative binding by g32P, as well as other single-stranded nucleic acid binding proteins (Kohwi-Shigematsu et al., 1978; Toulme & Helene, 1980; Kowalczykowski et al., 1981b, 1986). We present evidence that a 1:1 complex is formed and that the oligonucleotides bind in the ssDNA binding groove in g32P-(A+B) with a defined polarity of the phosphodiester backbone. Having shown this, we employ a complete series of oligonucleotide derivatives to map a set of two-dimensional distances between the metal ion [Co(II)] and a variably positioned nucleotide base in a series of protein–nucleic acid complexes.

[2] ϵA, 1,N^6-ethenoadenosine or 3-β-D-ribofuranosylimidazo[2,1-*i*]-purine; ϵA·HCl, 1,N^6-ethenoadenosine hydrochloride; ϵA-oligonucleotide, oligodeoxyribonucleotide containing a single 1,N^6-ethenoadenosine group.

Materials and Methods

Materials

All buffers were prepared from doubly distilled Milli-Q water by using reagent grade salts. Concentrated stock solutions of buffer salts were prepared and subjected to passage through Chelex-100 (Bio-Rad) to reduce the residual divalent metal ion concentration. An aqueous solution of chloroacetaldehyde was prepared by acidification of chloroacetaldehyde dimethyl acetal (Aldrich) in 50% sulfuric acid, followed by distillation and neutralization according to Secrist et al. (1972). Synthetic oligodeoxyribonucleotides were synthesized on an Applied Biosystems 380B automated synthesizer with phosphoramidite chemistry and were obtained in their deprotected and crude form. Trypsin and chromatographically purified DNAse were obtained from Sigma. *Crotalus durissis* phosphodiesterase was obtained from Boehringer-Mannheim (Indianapolis, IN).

Methods

Purification of g32P-(A+B). Gene 32 protein was purified according Giedroc et al. (1989), which describes tightly regulated temperature-inducible overexpression of the *gene 32* gene product from the phage λ P_L promoter. G32P was purified through the phenyl-Sepharose chromatography step, which results in a preparation free of detectable ssDNA endonuclease activities (Giedroc et al., 1990). This protein was then subjected to limited trypsinolysis to remove the terminal B and A domains and repurified to ≥99% homogeneity exactly as outlined (Giedroc et al., 1989). This material was then concentrated by ultrafiltration to ≈350 μM (Amicon) and dialyzed exhaustively (4 °C) into metal-free TNGa buffer (10 mM Tris-HCl, 0.1 M NaCl, 5% (v/v) glycerol, pH 8.0) and stored in 200-μL aliquots at −20 °C. G32P-(A+B) preparations contained stoichiometric Zn(II) by flame atomic absorption spectroscopy (Perkin-Elmer 2380). The Co(II)-substituted g32P-(A+B), prepared exactly as described (Giedroc et al., 1986), contained 0.95 mol of Co(II) by optical spectroscopy and flame atomic absorption spectroscopy and 0.07 mol of residual Zn(II) per mol of protein. For fluorescence titrations, g32P-(A+B) was subjected to further dialysis (4 °C) against T/0.1 M NaCl buffer (10 mM Tris-HCl, 0.1 mM Na_3EDTA, 0.1 M NaCl), aliquoted, and stored as described. The concentration of the g32P-(A+B) titrant was determined using ϵ_{282} = 41 300 $M^{-1}\cdot cm^{-1}$ (Spicer et al., 1979).

Preparation of 1,N^6-Ethenoadenylated Oligodeoxyribonucleotides. Crude synthetic oligonucleotides were resuspended in TE (10 mM Tris-HCl, 0.1 mM Na_3EDTA, pH 8.0), clarified by microcentrifugation, and desalted into water with a 1-mL Sephadex G-15C (Sigma) spun column. This material was taken to dryness and resuspended in aqueous chloroacetaldehyde at a concentration of ≈5 × 10^{-3} M adenosine residues. The reaction (Secrist et al., 1972; Tolman et al., 1974) was allowed to proceed for 24–36 h at 37 °C, until no further change in the optical spectrum was detectable. A 50–100 nmol portion of this material (4–5 preparative injections were typically required) was then directly loaded onto a reverse phase HPLC[1] column (Waters DeltaPak C18, 5-μm particle size, 300-Å pore size) equilibrated in 0.1 M triethylamine (Sigma) acetate, pH 6.5 (100% A) at 0.7 mL/min and ambient temperature. The column was developed with

an acetonitrile gradient [solvent B: 0.1 M triethylamine acetate, pH 6.5, 95% (v/v) acetonitrile] as described in the text. A Waters Powerline liquid chromatography system was employed with the flow rate and solvent composition maintained with a Waters 600E system controller. A Waters 490 multichannel detector was operated with simultaneous detection at 260 and 280 nm. The data were collected, digitized, integrated, and stored with the Waters Baseline software. The peak fractions identified as $1,N^6$-ethenoadenylated oligonucleotide by their absorption properties were pooled conservatively, dried, and resuspended in TE buffer. They were then desalted into T/0.1 M NaCl buffer through a G-15C spun column and stored at 4 °C. Rechromatography of all oligonucleotides generally indicated less than detectable levels of contaminating parent oligonucleotide (≤0.5%). No detectable cleavage or degradation of the purified ϵA-oligonucleotides even after a period of months at 4 °C was noted.

With these procedures, it was found that $1,N^6$-ethenoadenylation of crude oligonucleotides containing a terminal or penultimate 3′ adenosine residue resulted in formation of a major, apparently unmodified, oligonucleotide side product of shorter apparent chain length [cf. Tolman et al. (1974)]. However, when these crude oligonucleotides were first purified either via anion exchange (see below) or reverse-phase HPLC and subsequently reacted as above, there was no evidence of the presumptive hydrolysis reaction upon subsequent chromatography on the C18 column. Therefore, when purification was required or desired, the crude oligonucleotide preparation was subjected to anion-exchange HPLC on a Nucleogen DEAE 60-7 (Rainin) column optimized to obtain resolution of short oligonucleotides less then 10 nucleotides. The column was equilibrated (0.7 mL/min) with 100% A [20% (v/v) acetonitrile, 20 mM potassium phosphate, pH 7.2] and developed with a 0–75% B linear gradient (solvent B: solvent A plus 1 M KCl) run over 54 min, initiated 6 min post-injection. The column was then washed with 100% B and reequilibrated in 100% A prior to the next injection. Following chromatography, the peak fractions from multiple preparative runs (of ≈200 nmol each) were pooled conservatively, dialyzed exhaustively against 50 mM ammonium bicarbonate, and lyophilized to dryness. They were then treated with chloroacetaldehyde as detailed above.

Absorption Measurements. Absorption spectra of ϵA-oligonucleotides (2–5 μM oligonucleotide; 300 μL) were recorded on Hewlett-Packard 8452A UV-vis spectrophotometer at ambient temperature in T/0.1 M NaCl/1 mM magnesium acetate. Hydrolysis of oligonucleotides to mononucleotides *C. diurissis* phosphoesterase (10 μg/mL) was taken to be complete when the absorption spectrum ceased to change. The molar (oligonucleotide) extinction coefficients were estimated from the absorbance of the hydrolyzed mononucleotide constituents by using $\epsilon_{260} = 9200$ for thymidine monomers and $\epsilon_{260} = 5000$ for the ϵA monomer (Secrist et al., 1972). For the $l = 8$ oligonucleotides, the molar equivalent extinction coefficient of the hydrolyzed oligonucleotide, $\epsilon_{260,\text{hydrolyzed}} = (7 \times 9200) + 5000\ \text{M}^{-1}\cdot\text{cm}^{-1} = 6.94 \times 10^4\ \text{M}^{-1}\cdot\text{cm}^{-1}$. Similarly, for the $l = 6$ oligonucleotides, $\epsilon_{260,\text{hydrolyzed}} = (5 \times 9200) + 5000\ \text{M}^{-1}\cdot\text{cm}^{-1} = 5.1 \times 10^4\ \text{M}^{-1}\cdot\text{cm}^{-1}$. From these values the extent of hypochromism and molar extinction coefficients for the intact oligonucleotides were calculated to be $\epsilon_{260} = 6.25 \times 10^4\ \text{M}^{-1}(\text{oligonucleotide})\cdot\text{cm}^{-1}$ for the $l = 8$ oligonucleotides, while an $\epsilon_{260} = 4.59 \times 10^4\ \text{M}^{-1}(\text{oligonucleotide})\cdot\text{cm}^{-1}$ for the $l = 6$ oligonucleotides.

Fluorescence Measurements. All fluorescence measurements were made on an SLM 8000C spectrofluorometer. Q_o, the quantum yield of an ϵA-oligonucleotide, was calculated with (Brissette et al., 1989)

$$Q_o = Q_1/[(F_1/F_2)(A_2/A_1)] \quad (1)$$

F_1 and F_2 were quantitated from the fluorescence intensities at the same instrumental voltage and gain settings of a known concentration of oligonucleotide before (F_2) and following (F_1) complete hydrolysis with phosphodiesterase as described above [cf. Tolman et al. (1974)]. Since A_1 was found to be equal to A_2, where A is the absorbance at the excitation wavelength, eq 1 simplifies to $Q_o = Q_1/(F_1/F_2)$. $Q_1 = 0.56$, the quantum efficiency for ϵ-adenosine, was used for the $m = 0$ oligonucleotides while $Q_1 = 0.59$, the quantum efficiency for ϵ-ATP, was used for the calculation of Q_o for the internally labeled oligonucleotides (Secrist et al., 1972).

For ϵA-oligonucleotide titrations with protein, samples were prepared at the indicated concentration in 2.0 mL (1-cm path length) and were gently stirred continuously throughout the course of a titration with small (2–20 μL) aliquots of a concentrated stock solution of g32P-(A+B). Total dilution of the ϵA-oligonucleotide never exceeded 5%. The concentration of ϵA-oligonucleotide was determined directly on an aliquot of the fluorescence solution to be titrated. For these experiments, the ϵA fluorescence was monitored with an excitation wavelength (λ_{ex}) of 320 nm (2-nm band-pass) with the emission monochromater (λ_{em}) set at 401 nm (4-nm band-pass) at a 90° angle relative to the excitation light. The temperature was maintained in a thermostated sample compartment at 25 ± 0.1 °C. The measured fluorescence values at the jth addition of protein (F_j) were converted to corrected values ($F_{\text{corr},j}$) by first subtracting the background fluorescence of a buffer solution mock-titrated with protein. This fluorescence was then further corrected after accounting for dilution and inner filter effects [according to Birdsall et al. (1983)]. In all cases, the total absorbance of the solution was kept below 0.07 to minimize inner filter corrections. There was no evidence of photobleaching of the oligonucleotide under these conditions. The fluorescence or signal change is defined as $S_{\text{obs},j} = F_{j,\text{corr}}/F_{o,\text{corr}}$, the ratio of the corrected fluorescence obtained at the jth titration point to the free oligonucleotide fluorescence. For fluorescence enhancement, S_{obs} will be greater than 1.0; for fluorescence quenching, S_{obs} will be less than 1.0; this makes no difference in the analysis. S_{max} refers to the maximum extent of fluorescence enhancement (or quenching), which reflects 100% complex formation. Q_d, the quantum efficiency of the bound ϵA-oligonucleotide is calculated from $Q_d = Q_o S_{\text{max}}$. S_{max} values obtained by recording the relative fluorescence emission at a single emission wavelength for free and bound oligonucleotides (as in a typical titration) showed good agreement (within 5%) with that obtained by comparing the integrated areas of the fluorescence emission spectra of the free versus fully complexed ϵA-oligonucleotide, since the shape and maximum of the fluorescence emission spectra were not detectably different.

For titrations of a fixed concentration of g32P-(A+B) with a concentrated stock solution of oligonucleotide, the intrinsic protein fluorescence was quantitated upon excitation at 296 nm (1-nm bandwidth) with emission recorded at 347 nm (4-nm bandwidth), and the resulting data were analyzed as described (Giedroc et al., 1990).

Anisotropy Measurements. The steady-state fluorescence anisotropy of the ϵA-oligonucleotides was estimated under the solution conditions used to make the binding measurements. ϵA-oligonucleotide concentrations ranged from 2 to 8 μM. Glan–Thompson polarizers supplied with the instrument were used in the L format with total fluorescence emission (λ_{ex} =

Table I: Fluorescence Quantum Yields (Q_o, Q_d, and Q_{da}) and Equilibrium Binding Parameters (S_{max} and K_{obs}) of $l = 6$ and $l = 8$ 1,N^6-Ethenoadenylated Oligonucleotides for Zn(II) and Co(II) g32P-(A+B)[a]

m	ϵA-oligonucleotide	Q_o[b]	g32P-(A+B)	S_{max}[c]	Q_d[d]	Q_{da}[d]	K_{obs} ($M^{-1} \times 10^{-6}$)[c]
$l = 8$							
0	d[ϵA(pT)$_7$]	0.043 ± 0.001	Zn(II)	1.36 (±0.02)	0.059		1.5 (±0.4)
			Co(II)	0.77 (±0.01)		0.033	0.74 (±0.01)
1	d[TpϵA(pT)$_6$]	0.033 ± 0.001	Zn(II)	1.86 (±0.05)	0.061		0.33 (±0.07)
			Co(II)	1.29 (±0.01)		0.043	0.28 (±0.05)
3	d[(Tp)$_3$ϵA(pT)$_4$]	0.033	Zn(II)	3.68 (±0.10)	0.121		1.3 (±0.4)
			Co(II)	2.73 (±0.11)		0.090	0.83 (±0.03)
5	d[(Tp)$_5$ϵA(pT)$_2$]	0.034 ± 0.001	Zn(II)	3.46 (±0.20)	0.118		3.5 (±1.4)
			Co(II)	2.56 (±0.09)		0.087	1.3 (±0.2)
6	d[(Tp)$_6$ϵApT]	0.038 ± 0.002	Zn(II)	2.16 (±0.01)	0.082		3.5 (±0.3)
			Co(II)	1.56 (±0.02)		0.059	1.9 (±0.3)
7	d[(Tp)$_7$ϵA]	0.053 ± 0.002	Zn(II)	2.39 (±0.02)	0.127		3.1 (±0.7)
			Co(II)	1.42 (±0.05)		0.075	1.8 (±0.1)
$l = 6$							
0	d[ϵA(pT)$_5$]	0.046	Zn(II)	1.22 (±0.03)	0.056		0.12 (±0.01)
5	d[(Tp)$_5$ϵA]	0.047	Zn(II)	3.85 (±0.11)	0.181		0.11 (±0.01)

[a] Conditions: T/0.1 M NaCl, pH 8.1, 25 °C, λ_{ex} = 320 nm (2-nm band-pass), λ_{em} = 401 nm (4-nm band-pass). ϵA-oligonucleotide concentrations ranged from ≈6 × 10^{-7} to 1 × 10^{-5} M. The data are derived from at least two titrations with each ϵA-oligonucleotide at two concentrations. [b] From comparison of the integrated fluorescence intensities of ϵA-oligonucleotides before and after complete hydrolysis by phosphodiesterase (see Materials and Methods). The ϵA-oligonucleotide concentration ranged from 3 to 7 μM. [c] Binding parameters obtained as indicated in the legends to Figures 4 and 7. [d] Q_d (or Q_{da}) = $S_{max}Q_o$.

320 nm, 2-nm band-pass) recorded following passage through a Schott KV-389 long-pass filter. The polarization (P) and the anisotropy (r) of the samples were calculated from (Lakowicz, 1983)

$$P = (I_{VV} - GI_{VH})/(I_{VV} + GI_{VH}) \quad (2)$$

$$r = 2P/(3 - P) \quad (3)$$

where I_{VV} and I_{VH} are intensities of the emitted light polarized parallel and perpendicular, respectively, to the incident vertically polarized excitation beam. The factor $G = I_{HV}/I_{HH}$ corrects the measured intensities for differences in the sensitivity of the detection of vertically and horizontally polarized emitted light. For the instrumental configuration used in these studies, $G = 0.930 \pm 0.003$, indicative of well-collimated excitation and emission beams. Typically, 6–8 measurements of 20-s integration time each were collected and averaged for I_{VV}, I_{VH}, I_{HV}, and I_{HH} with any one oligonucleotide sample. The corrected intensities were obtained after subtraction of background intensities obtained with a buffer solution. Total ϵA-oligonucleotide fluorescence intensity was always 15-fold or more the background intensity of the buffer solution. The anisotropy of the oligonucleotide recorded after addition of g32P-(A+B) to both the buffer and oligonucleotide solutions sufficient to give >84% complex in the oligonucleotide solution (r_{obs}) was converted to $r_{complex}$, the anisotropy of the completely bound ϵA-oligonucleotide, from $r_{complex} = [\{(r_{obs} - r_{free})/f_{complex}\} - r_{obs} + r_{free} + r_{obs}\cdot(Q_d/Q_o)]\cdot(Q_o/Q_d)$, where $f_{complex}$ is the mole fraction of complexed oligonucleotide calculated from K_{obs} (cf. Table I).

Theory of Nonradiative Energy Transfer. Calculation of R_o and Distance (R) between the Donor and Acceptor. In the Förster theory (Förster, 1959) of nonradiative dipole–dipole energy transfer, the efficiency of energy transfer (E) from a donor to an acceptor is calculated from Q_d and Q_{da}, the quantum yields of the donor in the absence and presence of acceptor, respectively, from

$$E = 1 - (Q_{da}/Q_d) \quad (4)$$

E is related to separation of the donor and acceptor transition dipoles (R) according to the Förster relationship:

$$R = R_o(E^{-1} - 1)^{1/6} \quad (5)$$

where R_o is the critical distance or that which gives 50% transfer efficiency. R_o is related to the properties of the two chromophores by

$$R_o = (9.79 \times 10^3)(J\kappa^2\eta^{-4}Q_d)^{1/6}\ \text{Å} \quad (6)$$

J is the spectral overlap integral of the fluorescence emission spectrum of the donor with the absorption spectrum of the energy acceptor, evaluated from

$$J\ (M^{-1}\cdot cm^3) = \int F_d(\lambda)\epsilon_a(\lambda)\lambda^4\Delta\lambda / \int F_d(\lambda)\Delta\lambda \quad (7)$$

where $F_d(\lambda)$ and $\epsilon_a(\lambda)$ are the relative fluorescence intensity of the donor and the molar extinction coefficient ($M^{-1}\cdot cm^{-1}$) of the acceptor, respectively, and λ is the wavelength in nanometers. A summation was taken at 1-nm intervals, i.e., $\Delta\lambda = 1$ [cf. Wu and Tyagi (1987)]. κ^2 is a dynamic orientation factor that relates to the relative orientation and rotational freedom of the fluorescence emission and absorption dipoles of the donor and acceptor, respectively, during the excited state lifetime (see below). η is the refractive index of the medium surrounding donor and acceptor, taken to be 1.4, while Q_d is defined and determined as above.

Calculation of Maximum and Minimum Values of κ^2 from Fluorescence Anisotropy Measurements. For a donor and acceptor each characterized by a single transition dipole moment, a κ^2 value of $^2/_3$, the dynamic average, can only be applied when both species undergo isotropic rotation on the time scale of the fluorescent lifetime of the donor. Since the breadth of theoretically possible values of κ^2 ranges from 0 to 4, depending upon the polarization of each transition dipole, it is important to place limits on κ^2, which then allow one to place upper and lower limits on R_o, i.e., the uncertainty in the determination of R_o due only to the relative rotational freedom of both dipoles. Fortunately, in most cases with macromolecules, this case included, the donor and acceptor often show mixed polarizations across the spectral range over which energy transfer is predicted to occur. Rather than a single transition dipole, two or more incoherent dipoles may be present in one or both species. In the present donor/acceptor pair, the Co(II) LMCT region contains contributions from three S^-–Co(II) bonds, each of which has at least three electronic transitions (bonding and nonbonding) that polarize along three nearly perpendicular axes (Tennent & McMillin, 1979). As a result, there is essentially no uncertainty in κ^2 deriving from the acceptor Co(II) even if it is rotationally immobile (Haas et

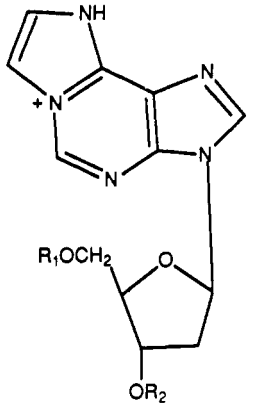

		R_1	R_2
l=8	m=0:	H	$(pT)_7$
	m=1:	Tp	$(pT)_6$
	m=3:	$(Tp)_3$	$(pT)_4$
	m=5:	$(Tp)_5$	$(pT)_2$
	m=6:	$(Tp)_6$	pT
	m=7:	$(Tp)_7$	H
l=6	m=0:	H	$(pT)_5$
	m=5:	$(Tp)_5$	H

FIGURE 1: General structure of 1,N^6-ethenoadenylated oligodeoxyribonucleotides used in this study. l = 6 or 8 while m = 0, 1, 3, 5, 6, or 7.

al., 1978; Chatterji et al., 1986). For the ϵA donor, polarization spectra of ϵA·HCl suggest depolarizing effects of multiple absorption dipoles, even on the long-wavelength side of the excitation spectrum (Secrist et al., 1972). However, the possibility exists in the present system, that *varying* degrees of polarized emission would occur in some ϵA-oligonucleotides relative to others. This might occur if a particular base is more rigidly held in the complex and hindered in its rotation on the time scale of excitation relative to another. Dale et al. (1979) have shown that measurement of the fluorescence anisotropies of both the donor and acceptor (only the donor in this case) can be used to place limits on the value of κ^2. Anisotropies of the bound oligonucleotide were determined as described above. The average depolarization factor $\langle d_D \rangle$ is related to the anisotropy (r) by

$$\langle d_D \rangle = r/0.4 = \langle d_D^x \rangle^2 \quad (8)$$

Maximum and minimum values of $\langle \kappa^2 \rangle$ are then given by (Dale et al., 1979; Gettins et al., 1990)

$$\langle \kappa^2 \rangle_{max} = 2/3(1 + \langle d_D^x \rangle + \langle d_A^x \rangle + 3\langle d_D^x \rangle \langle d_A^x \rangle) \quad (9)$$

$$\langle \kappa^2 \rangle_{min} = 2/3[1 - (\langle d_D^x \rangle + \langle d_A^x \rangle)/2] \quad (10)$$

where $\langle d_D^x \rangle$ and $\langle d_A^x \rangle$ are the axial depolarization factors for the donor (D) and acceptor (A), respectively. Here, $\langle d_A^x \rangle$ was set equal to zero for reasons discussed above. From these maximum and minimum values of $\langle \kappa^2 \rangle$, maximum and minimum values of R_0 can be calculated according to

$$R_{0,max} = (1.5\langle \kappa^2 \rangle_{max})^{1/6} R_0 \text{ (isotropic)} \quad (11)$$

$$R_{0,min} = (1.5\langle \kappa^2 \rangle_{min})^{1/6} R_0 \text{ (isotropic)} \quad (12)$$

Finally, the maximum and minimum values of R_0 are then used to calculate the minimum and maximum values of R with eq 5.

RESULTS

1,N^6-Ethenoadenylation of Adenine-Containing Oligodeoxyribonucleotides. The general structure of 1,N^6-ethenoadenylated oligonucleotides is shown in Figure 1. Crude oligodeoxyribonucleotides of defined sequence (5′ → 3′) d-[$(Tp)_m$A$(pT)_{l-m-1}$] where $0 \leq m \leq l-1$, containing a single adenosine were desalted into H_2O, dried, and dissolved in aqueous chloroacetaldehyde at pH 4.5 at $\approx 5 \times 10^{-3}$ M adenosine residues. The reaction was allowed to proceed for 24–36 h (37 °C), after which time the reaction products were loaded directly onto a C18 reverse-phase high-pressure liquid chromatography column equilibrated with 0.1 M triethylamine acetate, pH 6.5, at ambient temperature. As shown in Figure 2, an 11–12% linear acetonitrile gradient over 30 min effects

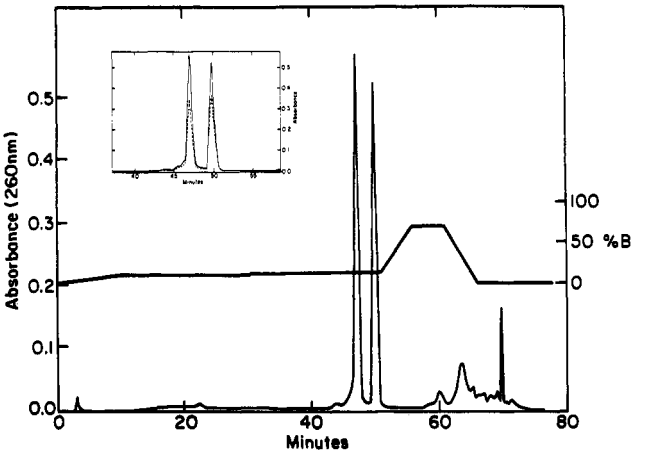

FIGURE 2: Reverse-phase HPLC of a mixture of unmodified parent d[A$(pT)_7$] and 1,N^6-ethenoadenylated [ϵA$(pT)_7$] octanucleotides. The absorbance was monitored at both 260 and 280 nm as indicated. The solvent composition was varied as shown by the %B mixed with the A solvent to obtain 100% total (A + B) solvent composition. See Materials and Methods for other details.

baseline separation of the parent unmodified oligonucleotide (47 min) and the ϵA-oligonucleotide derivative (50 min). Although these reaction conditions generally give >90% ethenoadenylation of the oligonucleotide, Figure 2 shows a representative chromatogram of a d[A$(pT)_7$]/d[ϵA$(pT)_7$] mixture (l = 8) to better illustrate the quality of the separation. In a representative l = 6 mixture, d[A$(pT)_5$] and d[ϵA$(pT)_5$] eluted at 38 and 45 min under the same chromatographic conditions. Note that these conditions effectively remove any ϵA-mononucleoside (or ϵA-mononucleotide) impurity in addition to oligonucleotide contaminants of shorter length present in the original preparation. Following a final desalting into binding buffer, typical yields of ≥99% homogeneous ϵA-oligonucleotides ranged from 20 to 30% on the basis of starting crude OD units.

Spectroscopic Characterization. The UV absorption spectrum of a representative l = 8 ϵA-oligonucleotide [ϵA-$(pT)_7$] shows a long-wavelength band in the near ultraviolet [$\epsilon_{310} \approx 2.9 \times 10^3$ M (oligonucleotide)$^{-1}$·cm^{-1}] and a shoulder at 276 nm, both of which arise from the ϵA base (Secrist et al., 1972) (data not shown). The absorption maximum is red-shifted to 267 nm [$\epsilon_{267} = 7.0 \times 10^4$ M (oligonucleotide)$^{-1}$·cm^{-1}], and the $\epsilon_{280}/\epsilon_{260}$ ratio is reduced relative to the unmodified oligonucleotide, the latter fact facilitating purification by HPLC (Figure 2, inset). Identical trends are observed for the ϵA-hexanucleotides (data not shown). Enzymatic hydrolysis of the both d[A$(pT)_7$] and d[ϵA$(pT)_5$] to the ϵA-mononucleoside and thymidine 5′-monophosphate monomers by the exonuclease snake venom phosphodiesterase reveals a ≈10% hypochromism at 260 nm associated with both oligonucleotides, as expected from previous studies (Tolman et al., 1974).

The corrected fluorescence excitation and emission spectra of all 1,N^6-ethenoadenylated oligonucleotides are essentially superimposable and comparable as a group to published spectra of the monomer ϵA·HCl[2] (Secrist et al., 1972). Representative fluorescence emission and excitation spectra are shown in Figure 3 for d[ϵA$(pT)_7$]; these spectra demonstrate that the sole contributor to the ϵA-oligonucleotide fluorescence in the 400-nm region is the ϵA-base. In accordance with the absorption measurements and previous studies with ϵA-dinucleoside monophosphates (Tolman et al., 1974), the fluorescence quantum yields (Q_0) of all ϵA-oligonucleotides are greatly reduced relative to ϵATP (Q_0 = 0.59).

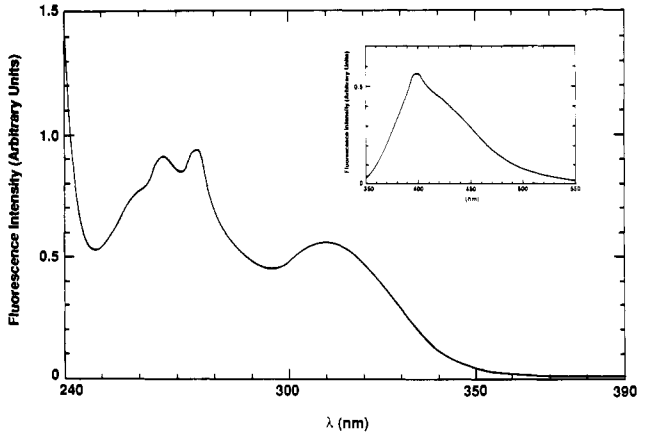

FIGURE 3: Fluorescence spectroscopic characteristics of a representative $l = 8$ ϵA-oligonucleotide. Excitation spectra of 4.28×10^{-6} M d-[ϵA(pT)$_7$], λ_{em} = 401 nm (4-nm band-pass). (Inset) Emission spectrum of d[ϵA(pT)$_7$], λ_{ex} = 320 nm (2-nm band-pass). Conditions: T/0.1 M NaCl, 25 °C.

In fact, Q_o for all ϵA-oligonucleotides from length $l = 6$ to 8 nucleotides varies from 0.033 to 0.053 (Table I). Oligonucleotides containing either a 5′ or 3′-terminal ϵA-base have a slightly larger Q_o value relative to those that have an internally positioned probe. As expected (Tolman et al., 1974), the severe quenching of the ϵA fluorescence which accompanies incorporation of the ϵA-base into an oligonucleotide is completely relieved upon hydrolysis to constituent monomer units with snake venom phosphodiesterase (data not shown).

The Binding of ϵA-Oligonucleotides to g32P-(A+B) Is Polar with Respect to Phosphodiester Chain Direction. In order for site-specifically labeled ϵA-oligonucleotides to be useful as reporter groups of the immediate binding site environment in the protein–nucleic acid complex, it must be demonstrated that (1) a 1:1 protein–nucleic acid complex is formed, and (2) the oligonucleotide binds with a fixed polarity of the phosphodiester backbone on the protein. In addition, it would be desirable that 1,N^6-ethenoadenylation of the oligonucleotide have little discernable effect on binding affinity of a nucleotide chain of sufficient length to establish all protein–nucleic acid contacts. The gene 32 protein derivative used in these studies is the DNA-binding core fragment, termed g32P-(A+B),[1] since in contrast to the intact protein, this molecule is essentially monomeric over the concentration range used in the present study (Giedroc et al., 1990).

To establish a polarity in the binding site, we carried out equilibrium binding studies with two pairs of oligonucleotides with inverted polarities. One pair are octanucleotides ($l = 8$) where $m = 0$ {d[ϵA(pT)$_7$]} and $m = 7$ {d[(Tp)$_7$ϵA]}, while the other pair are hexanucleotides ($l = 6$) where $m = 0$ {d[ϵA-(pT)$_5$]} and $m = 5$ {d[(Tp)$_5$ϵA]}. Although most previously published data provide evidence for a 1:1 stoichiometry in the g32P-(A+B)–octanucleotide system [cf. Karpel (1990)], we first performed equilibrium binding measurements with d-[(Tp)$_7$ϵA] and Zn(II) g32P-(A+B) at two different total concentrations of oligonucleotide to verify this in our experimental system (data not shown). Quantitative analysis of these data [cf. Bujalowski and Lohman (1989)] reveals that the relationship between the average number of g32P-(A+B) molecules bound per oligonucleotide and signal change is linear and saturates at a stoichiometry of 1:1 (data not shown). All subsequent titrations were analyzed with the assumption that the 1:1 stoichiometry and a linear relationship between the degree of binding and signal change (i.e., $\sum \nu_i = P_{bound}/D_t = D_{bound}/D_t = S_{obs}/S_{max}$) obtained for d[(Tp)$_7$ϵA] holds for all ϵA-oligonucleotides.

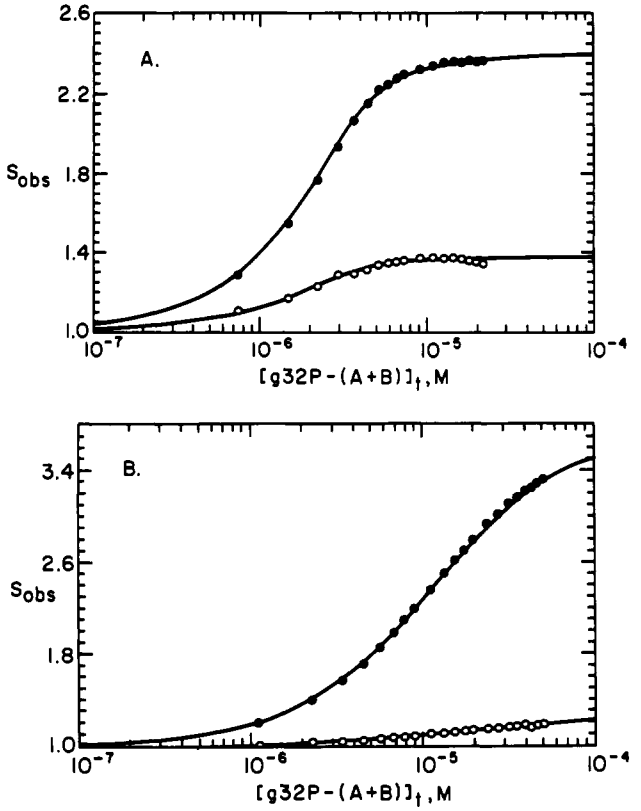

FIGURE 4: (A) Differential enhancement of the ϵA fluorescence of two $l = 8$ ϵA-oligonucleotides, d[ϵA(pT)$_7$] (○) and d[(Tp)$_7$ϵA] (●), upon binding by Zn(II) g32P-(A+B) (λ_{ex} = 320 nm; λ_{em} = 401 nm). $S_{obs} = 1.0$ defines the normalized free ϵA-oligonucleotide fluorescence (see Materials and Methods). Oligonucleotide concentrations were 2.53×10^{-6} M d[ϵA(pT)$_7$] and 2.97×10^{-6} M d[(Tp)$_7$ϵA]. The solid lines represent theoretical isotherms expected for a 1:1 stoichiometry as dictated by the following equation: $P_t = (S_{obs}/S_{max})\{1/[K_{obs}[1 - (S_{obs}/S_{max})]] + D_t\}$ where P_t is total protein titrant and D_t is the total oligonucleotide concentration. They are defined by the following parameters: d[(Tp)$_7$ϵA], $K_{obs} = 2.40 \times 10^6$ M^{-1}, $S_{max} = 2.40$; d-[ϵA(pT)$_7$], $K_{obs} = 1.82 \times 10^6$ M^{-1}, $S_{max} = 1.38$. (B) Differential enhancement of the ϵA fluorescence of two $l = 6$ oligonucleotides, d[ϵA(pT)$_5$] (○) and d[(Tp)$_5$ϵA] (●) upon binding by Zn(II) g32P-(A+B). Oligonucleotide concentrations were 1.058×10^{-5} M d[ϵA(pT)$_5$] and 5.05×10^{-6} M d[(Tp)$_5$ϵA]. The solid lines are defined by the following parameters: d[(Tp)$_5$ϵA], $K_{obs} = 1.1 \times 10^5$ M^{-1}, $S_{max} = 3.65$; d[ϵA(pT)$_7$], $K_{obs} = 1.1 \times 10^5$ M^{-1}, $S_{max} = 1.222$.

Figure 4A shows that when two symmetric ϵA-octanucleotides, d[ϵA(pT)$_7$] and d[(Tp)$_7$ϵA] are titrated with g32P-(A+B) at approximately 3 μM total ϵA-oligonucleotide, the S_{max} values obtained for each oligonucleotide are significantly different from one another, 1.38 for d[ϵA(pT)$_7$] relative to 2.40 with d[(Tp)$_7$ϵA]. However, the measured K_{obs} estimated from the best-fit theoretical isotherms are similar, 1.82×10^6 M^{-1} vs 2.40×10^6 M^{-1} for d[ϵA(pT)$_7$] and d[(Tp)$_7$ϵA], respectively (Table I). Q_d, the quantum efficiency of the complexed oligonucleotide, was found to be 0.059 and 0.127 for d[ϵA(pT)$_7$] and d[(Tp)$_7$ϵA], respectively.

Figure 4B shows the analogous experiment with the $l = 6$ oligonucleotides with the ϵA moiety symmetrically positioned at either the 5′ {d[ϵA(pT)$_5$]} or the 3′ {d[(Tp)$_5$ϵA]} ends. The result is even more striking here. Once again, both titrations are described by the same K_{obs}, 1.1×10^5 M^{-1}, some ≈20-fold reduced relative to the corresponding octanucleotides, and a 1:1 stoichiometry. However, $S_{max} = 1.22$ for d[ϵA(pT)$_5$] while $S_{max} = 3.75$ for d[(Tp)$_5$ϵA], corresponding to Q_d values of 0.056 and 0.181, respectively (Table I). These data establish that the binding of oligonucleotides of $l = 6$ or 8 by g32P-(A+B) is *polar* with respect to the binding site. They also

Table II: Equilibrium Binding Parameters for 1,N^6-Ethenoadenylated and Corresponding Unmodified Parent Oligonucleotides for g32P-(A+B)[a]

oligonucleotide	$K_{obs} \times 10^{-6}$ (M^{-1})	Q_{max}	$Q_{max,\epsilon A}/Q_{max,A}$
d[ϵA(pT)$_7$]	0.9 (±0.2)	0.361 (±0.005)	0.99
d[A(pT)$_7$]	1.2 (±0.4)	0.365 (±0.001)	
d[TpϵA(pT)$_6$]	0.5 (±0.2)	0.385 (±0.005)	1.08
d[TpA(pT)$_6$]	0.5 (±0.2)	0.358 (±0.001)	
d[(Tp)$_3\epsilon$A(pT)$_4$]	1.5 (±0.1)	0.439 (±0.004)	1.14
d[(Tp)$_3$A(pT)$_4$]	1.2 (±0.1)	0.385 (±0.001)	
d[(Tp)$_5\epsilon$A(pT)$_2$]	1.9 (±0.1)	0.439 (±0.001)	1.37
d[(Tp)$_5$A(pT)$_2$]	1.3 (±0.1)	0.321 (±0.001)	
d[(Tp)$_6\epsilon$ApT]	1.9 (±0.4)	0.44 (±0.01)	1.43
d[(Tp)$_6$ApT]	0.8 (±0.1)	0.31 (±0.01)	
d[(Tp)$_7\epsilon$A]	1.8 (±0.5)	0.468 (±0.003)	1.23
d[(Tp)$_7$A]	1.0 (±0.4)	0.379 (±0.004)	

[a] Derived from experiments like those shown in Figure 5. The g32P-(A+B) concentration ranged from 2.5×10^{-7} to 1.05×10^{-6} M. At least two independent determinations were made for each oligonucleotide.

demonstrate that loss of two nucleotides from an octanucleotide results in the loss of one or more intermoleclar contacts.[3]

Positional Effects of the ϵA Moiety on the Intrinsic Fluorescence Emission of g32P-(A+B) in the Protein–ssDNA Complex. Another series of equilibrium binding measurements were made by monitoring the quenching of the intrinsic protein fluorescence upon binding oligonucleotides. The relative maximal extent of fluorescence quenching (Q_{max}) is dictated by both base and sugar composition and sequence of the nucleic acid molecule. Two parallel titrations performed with the unlabeled parent oligonucleotide vs the corresponding 1,N^6-ethenoadenylated oligonucleotide will reveal any positional influence, e.g., in K_{obs} or Q_{max}, of the ϵA moiety. Specifically, if a proximate Trp side chain(s) closely approaches an ϵA-base(s), singlet–singlet energy transfer can potentially occur from the indole ring to the ϵA ring due to the spectral overlap between the emission spectrum of Trp and the absorption spectrum of ϵA (Gruber & Leonard, 1975; Ledneva et al., 1978; Toulme & Helene, 1980). The efficiency of energy transfer is a function of the two-dimensional distance between the Trp donor and ϵA acceptor.[4] In the event of such energy transfer in g32P, *quenching* of the total Trp fluorescence will result upon binding the ϵA-oligonucleotide to an extent *greater* than that which would occur with the corresponding unlabeled oligonucleotide of otherwise identical primary structure (Ledneva et al., 1978; Toulme & Helene, 1980).

In Figure 5, each panel shows a representative titration of g32P-(A+B) with one of the six $l = 8$ ϵA-oligonucleotides (A, $m = 0$; and B, $m = 7$) compared with a titration carried out with the parent unlabeled oligonucleotide of the same sequence. Identical experiments were carried out with the all six $l = 8$ ϵA-oligonucleotides to determine the effect of the ϵA moiety as it is moved systematically from the 5′ to the 3′ end of the bound oligonucleotide (Table II). The relative efficiency of energy transfer from a Trp side chain(s) can be approximated by a comparison of the relative magnitudes of Q_{max} recorded

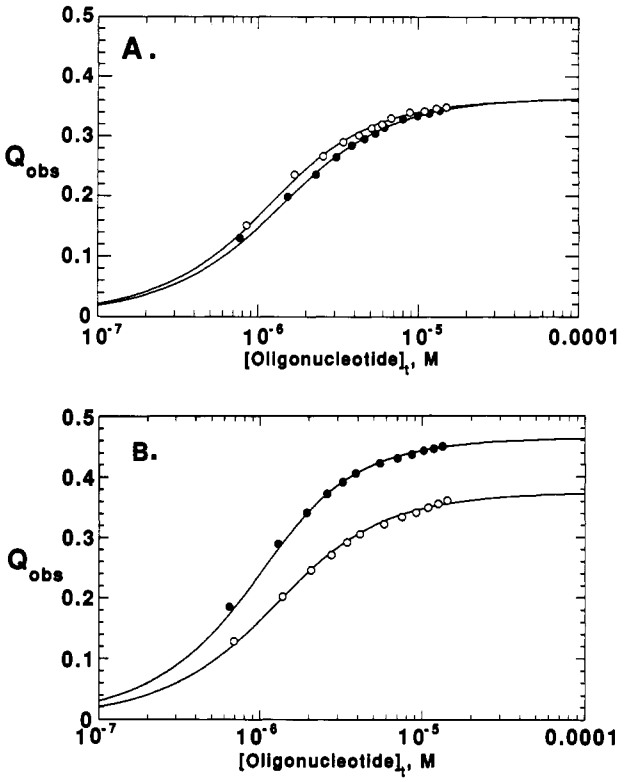

FIGURE 5: Differential quenching of the intrinsic fluorescence of Zn(II) g32P-(A+B) upon binding to a 1,N^6-ethenoadenylated oligonucleotide (filled symbols) compared to the corresponding unlabeled parent oligonucleotide (open symbols) of the same sequence (λ_{ex} = 296 nm; λ_{em} = 347 nm). $Q_{obs} = 0$ defines the normalized free protein fluorescence (see Materials and Methods). In all titrations, the concentration of g32P-(A+B) was 1.05×10^{-6} M. The solid lines drawn through the experimental points represent the best two-parameter (Q_{max} and K_{obs}) fit that describes a theoretical isotherm of the following equation: $D_t = (Q_{obs}/Q_{max})\{1/[K_{obs}[1 - (Q_{obs}/Q_{max})]] + P_t\}$. These best-fit Q_{max} and K_{obs} (M^{-1}) values, respectively, are indicated in parentheses following the oligonucleotide designation. (A) d[ϵA(pT)$_7$] ($m = 0$) (0.366; 1.16×10^6) and d[A(pT)$_7$] (0.364; 1.6×10^6); (B) d[(Tp)$_7\epsilon$A] ($m = 7$) (0.465; 2.3×10^6) and d[(Tp)$_7$A] (0.375; 1.4×10^6). The mean values for Q_{max} and K_{obs} obtained from replicate titrations and analogous titrations carried out for all other $l = 8$ oligonucleotides are compiled in Table II.

in the presence (ϵA-oligonucleotide) and absence (unlabeled oligonucleotide) of the putative energy acceptor, i.e., $Q_{max,\epsilon A}/Q_{max,A}$. It is clear that a Trp side chain(s) is (are) positioned closest to the ϵA base to or between nucleotide residues 6 and 7 (from the 5′ end) in the octanucleotide, since energy transfer appears most efficient here (Table II). The 3′-terminal, fourth, second, and 5′-terminal ϵA-bases appear incrementally further removed from the Trp(s) to the point where the 5′-terminal ϵA-base, relative to A, affects the intrinsic protein fluorescence of the complex to a negligible extent (Figure 5A).[5]

[3] Quantitative salt-induced dissociation experiments suggest the reduction in binding free energy that characterizes hexanucleotide vs octanucleotide binding to the core fragment is derived from a reduction in both electrostatic and nonelectrostatic free energy terms (D.G., unpublished).

[4] Calculation of an energy transfer efficiency between a unique donor-acceptor pair is not possible since one or more of the five tryptophans in g32P-(A+B) can potentially function as energy donor(s) to the bound nucleic acid.

[5] Direct demonstration of Trp → ϵA energy transfer (Lakowicz, 1983) in this system is technically complicated by the low fluorescence quantum yield of the ϵA-oligonucleotide relative to Trp fluorescence of g32P. Any set of solution conditions that gives acceptable levels of complex formation places the fluorescence emission of the oligonucleotide as a shoulder on the low-energy side of the g32P emission spectrum. We have found, however, that when g32P-(A+B)–d[(Tp)$_7\epsilon$A] ($m = 7$) complex formation is monitored at ϵA-oligonucleotide fluorescence emission (430 nm) with excitation of both Trp and d[(Tp)$_7\epsilon$A] (298 nm), the corrected enhancement of the ϵA-oligonucleotide fluorescence (S_{max}) is ≈22% larger than when the ϵA-oligonucleotide is selectively excited (325 nm) (D.G. and R.K., unpublished). Analogous experiments with d[ϵA(pT)$_7$] ($m = 0$) fail to yield the same result. These observations are consistent with energy transfer from a Trp donor(s) to the ϵA acceptor in d-[(Tp)$_7\epsilon$A], but not in d[ϵA(pT)$_7$].

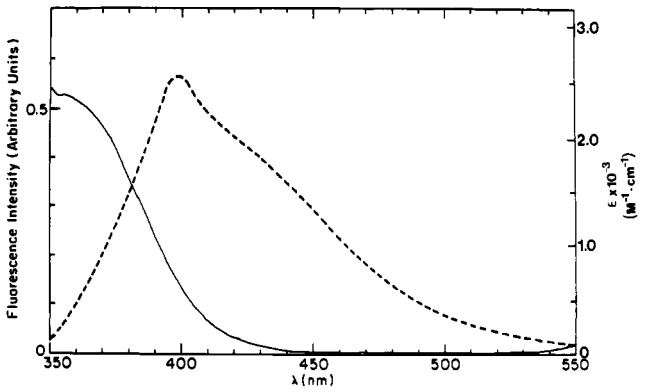

FIGURE 6: Spectral overlap between the fluorescence emission spectrum of an ϵA-oligonucleotide, d[ϵA(pT)$_7$] (λ_{ex} = 320 nm) (---), and the LMCT region of the absorption spectrum of Co(II)-substituted g32P-(A+B) (—). The spectral overlap integral was calculated to be 1.483 × 10^{-15} M^{-1}·cm^3 (see Materials and Methods). Conditions: T/0.1 M NaCl, pH 8.1, 25 °C.

These data provide independent evidence that all ϵA-oligonucleotides bind with a singular polarity of the phosphodiester chain and that the 5′ and 3′ ends of the oligonucleotide define structurally distinct microenvironments. It is also apparent (Table II) that the etheno moiety has little influence on the magnitude of K_{obs} of g32P-(A+B) for any l = 8 oligonucleotide, further support that the uniquely positioned 1,N^6-ethenoadenosine moiety can be considered a truely nonperturbing spectroscopic probe.

The Fluorescence Emission Spectrum of an ϵA-Oligonucleotide Overlaps the Absorption Spectrum of Co(II)-Substituted g32P-(A+B). Co(II) is an excellent metal ion substitute for the intrinsic Zn(II) in g32P as it induces little significant perturbation in the structure of the g32P monomer as evidenced by a variety of physicochemical criteria (Coleman & Giedroc, 1989). The Co(II) is bound to the ssDNA-binding core fragment through three Cys S^- atoms and a fourth non-sulfur donor (Giedroc et al., 1986, 1989). The optical absorption spectrum contains, in addition to ligand field "d–d" transitions of the high spin d^7 Co(II) ion in the visible region, two resolvable $S^- \rightarrow$ Co(II) ligand-to-metal charge transfer (LMCT) transitions in the near UV, indicative of coordination to Cys sulfur (Giedroc et al., 1986). As shown in Figure 6, the fluorescence emission spectrum of the ϵA-oligonucleotide d[ϵA(pT)$_7$] overlaps the LMCT region of the Co(II) absorption spectrum. This degree of spectral overlap ensures that the ϵA-base is potentially useful as a fluorescence energy donor with the Co(II) LMCTs participating as energy acceptors in Förster-mediated nonradiative energy transfer (Förster, 1959). The fluorescence emission spectra of all ϵA-oligonucleotides are superimposable under the same solution conditions, regardless of the position of the base in the primary structure. Moreover, the shape of the Co(II) absorption and the oligonucleotide fluorescence emission spectra do not change appreciably upon complex formation (Giedroc et al., 1989; data not shown), permitting the same value of J, the spectral overlap integral, to be used to evaluate all ϵA-Co(II) intermolecular distances.

The Binding of (l = 8) ϵA-Oligonucleotides Exhibits Distinguishable Fluorescence Properties Dependent on the Value of m. In the previous section, we examined the equilibrium binding to the core fragment of two terminally labeled l = 8 oligonucleotides with inverted polarities, m = 0 d[ϵA(pT)$_7$] and m = 7 d[(Tp)$_7$ϵA], by titrating the oligonucleotides with Zn(II) g32P-(A+B) while monitoring complex formation at the steady-state ϵA-oligonuleotide fluorescence. In these two

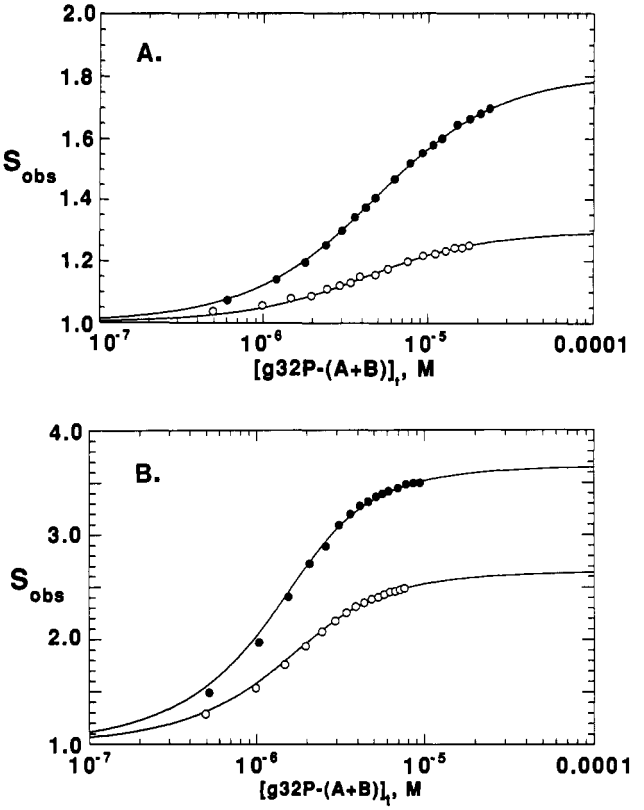

FIGURE 7: Enhancement of the fluorescence of two, 1,N^6-ethenoadenylated oligodeoxyribonucleotides upon binding by Zn(II) g32P-(A+B) (●) and Co(II) g32P-(A+B) (○) (λ_{ex} = 320 nm; λ_{em} = 401 nm). S_{obs} = 1.0 is the free normalized ϵA-oligonucleotide fluorescence. The solid lines are theoretical isotherms that *assume* a 1:1 stoichiometry. Following the oligonucleotide designation and the metallated form of the protein used are the oligonucleotide concentration (M), and best-fit S_{max} and K_{obs} (M^{-1}) values, respectively, for that particular titration. (A) d[TpϵA(pT)$_6$] (m = 1), Zn(II); 2.47 × 10^{-6}, 1.81, 2.84 × 10^5); Co(II): 2.47 × 10^{-6}, 1.30, 3.37 × 10^5; (B) d[(Tp)$_5$ϵA(pT)$_2$] (m = 5), Zn(II): 1.81 × 10^{-6}, 3.66, 2.15 × 10^6; Co(II): 1.81 × 10^{-6}, 2.65, 1.54 × 10^6. The analysis of these and analogous titrations carried out with all other l = 8 oligonucleotides are compiled in Table I. Conditions: T/0.1 M NaCl, pH 8.1, 25 °C.

cases, Q_d, the quantum yield in the *absence* of nonradiative energy transfer to Co(II), was found to be 0.059 and 0.127, for d[ϵA(pT)$_7$] and d[(Tp)$_7$ϵA], respectively (Table I). Exactly analogous titrations carried out with the Co(II)-substituted g32P-(A+B) allow a determination of Q_{da}, the quantum efficiency in the presence of energy transfer, in addition to K_{obs} for Co(II) g32P-(A+B).

In Figure 7 are shown representative titrations obtained with two of the six ϵA-octanucleotides (m = 1 and m = 5), which place the ϵA moiety at the second (panel A) and sixth (panel B) positions relative to the 5′ end of the l = 8 oligonucleotide. Each panel shows one titration with Zn(II) g32P-(A+B) (in the absence of energy acceptor) and one with the Co(II)-substituted protein (in the presence of energy transfer acceptor), under the same solution conditions and similar concentrations of ϵA-oligonucleotide. Table I summarizes the analysis of analogous equilibrium binding isotherms generated for all l = 8 ϵA-oligonucleotides.

Inspection of Table I reveals that the maximal extent of fluorescence enhancement (S_{max}) obtained with the native Zn(II) protein varies with the position of the ϵA moiety in the primary structure, or m. For example, with the m = 3 and m = 5 (cf. Figure 7B) oligonucleotides, S_{max} values reach 3.68 and 3.74, respectively, while for the m = 0 oligonucleotide (cf. Figure 4A), S_{max} = 1.36. In addition, in every case, S_{max} in

Table III: Energy Transfer Efficiencies (E), Critical Förster Distances [R_0 (Isotropic)], and Distances [R (Isotropic)] from the Co(II) to the 1,N^6-Ethenoadenylate Moiety in g32P-(A+B)–ϵA-Oligonucleotide Complexes[a]

ϵA-oligonucleotide	E[b]	R_0 (Å)[b]	R (Å)[c]
d[ϵA(pT)$_7$]	0.43 (±0.02)	15.3	16.0 (15.9–16.2)
d[TpϵA(pT)$_6$]	0.31 (±0.02)	15.5	17.7 (17.5–18.0)
d[(Tp)$_3$ϵA(pT)$_4$]	0.26 (±0.05)	17.3 (±0.1)	20.7 (19.9–21.6)
d[(Tp)$_5$ϵA(pT)$_2$]	0.26 (±0.06)	17.2 (±0.1)	20.5 (19.7–21.8)
d[(Tp)$_6$ϵApT]	0.28 (±0.01)	16.2	19.0 (18.9–19.2)
d[(Tp)$_7$ϵA]	0.41 (±0.01)	17.4	18.6 (18.3–18.9)

[a] Calculated with the data in Table I assuming an isotropic orientation factor, $\langle\kappa^2\rangle$ = 0.667, and η = 1.4 (see Materials and Methods). [b] The uncertainty in E incorporates the standard error in S_{max} obtained in the presence and absence of acceptor (Table I). If no uncertainty is given for R_0, it is less than 0.1 Å. [c] The range given reflects the uncertainty associated with E.

the presence of energy acceptor [with the Co(II) protein] is significantly lower than that obtained in the absence of energy acceptor [with the Zn(II) protein]. Thus, $Q_d > Q_{da}$ in all cases, evidence that the donor and acceptor are in range of the critical Förster distance in all Co(II) g32P-(A+B)–ϵA-oligonucleotide complexes. The fluorescence of the bound oligonucleotide in the presence and absence of energy acceptor was completely reversible to uncomplexed levels upon dissociation of the complex with incremental addition of NaCl (data not shown).

The K_{obs} values determined for the native Zn(II) and Co(II)-substituted core fragment on all ϵA-oligonucleotides (Table I) reveal that the Co(II) protein binds with a moderately lower binding affinity in some cases, ranging from ≈1.5- to 2-fold reduced from the Zn(II) protein under identical solution conditions. This suggests that substitution of Zn(II) for Co(II) alters to some extent the properties of the complex. Interestingly, K_{obs} increases moderately as the ϵA-base is moved from the 5′ to the 3′ end of the oligonucleotide, a trend observed for *both* the Zn(II) and Co(II) proteins (see also Table II). Thus, although not necessarily identical, the individual complexes formed in the presence and absence of the energy acceptor are structurally similar.

Distance Relationships Calculated from the Energy Transfer Efficiencies. The energy transfer efficiences and corresponding values of R_0(isotropic), the critical distance at which E = 0.5, and R (isotropic), the actual distance between donor and acceptor obtained for the each of the six l = 8 ϵA-oligonucleotides are summarized in Table III with κ^2 set to 0.667 (see Materials and Methods). The values of R_0 vary from 15.3 to 17.4 Å, depending primarily on the value of Q_d, the quantum yield of the completely complexed ϵA-oligonucleotide (Table I). The energy transfer efficiences (E) vary from a high of 0.43 for the m = 0 oligonucleotide and a low of 0.26 obtained for both internally labeled m = 3 and m = 5 ϵA-oligonucleotides. The actual donor–acceptor distances vary from 16.0 to 20.7 Å among all ϵA-oligonucleotides, with the intrinsic Co(II) relatively closer to *both* the 5′ and 3′ ϵA-bases than it is to internally positioned ϵA moieties.

Steady-State Fluorescence Anisotropy of the ϵA-Base in Protein–Oligonucleotide Complexes as a Function of m. Steady-state fluorescence anisotropy measurements of ϵA-oligonucleotides can yield insight into the relative rotational mobility of the ϵA-base during the excited-state lifetime (Lakowicz, 1983). Steady-state fluorescence anisotropies (r_{free}) were determined for all ϵA-oligonucleotides under solution conditions of the binding experiment (Table IV). Among the l = 8 oligonucleotides, r_{free} reaches a maximum value, or lowest rotational mobility, for the internally positioned bases in d[(Tp)$_3$ϵA(pT)$_4$] and d[(Tp)$_5$ϵA(pT)$_2$]. Lower r_{free} values, and thus greater motility, occurs to equal extents as the ϵA-base is moved to the 5′ and 3′ ends of the oligonucleotide. These relatively low anisotropies are not unexpected from published polarization spectra of ϵA·HCl (r < 0.04 at 21 °C) (Secrist et al., 1972).

This trend in r_{free} contrasts with anisotropies determined for the protein–nucleic acid complexes ($r_{complex}$) (Table IV), which are more similar than different for all oligonucleotides of m > 0 (see Discussion). The magnitudes of $r_{complex}$, estimated under conditions of energy transfer, can be used to place limits on the uncertainty in the determination of R_0 for that oligonucleotide, and thus R, deriving exclusively from the uncertainty in κ^2, the orientation factor (Dale et al., 1979; Gettins et al., 1990) (see Materials and Methods) (Table IV). Individual mean values of $r_{complex}$ were thus used to estimate the axial depolarization of the donor fluorescence emission of each protein–oligonucleotide complex, which relates to the maximum (κ^2_{max}) and minimum (κ^2_{min}) values of the orientation factor, calculated with eqs 9–10 (Table IV). These values in

Table IV: Fluorescence Anisotropies (r_{free} and $r_{complex}$) and Orientational Analysis of g32P-(A+B)–1,N^6-Ethenoadenylated Oligonucleotide Complexes and Calculation of R_0 and R[a]

ϵA-oligonucleotide	r_{free}	$r_{complex}$		$\langle d_D\rangle$[b]	$\langle d_D{}^x\rangle$	$\langle\kappa^2\rangle$	R_0 (Å)	R (Å)
d[ϵA(pT)$_7$]	0.019	0.054	minimum	0.135	0.367	0.544	14.8	15.5
(m = 0)	(±0.003)[c]	(±0.002)[c]	isotropic			0.667	15.3	16.0
			maximum	0.135	0.367	0.911	16.1	16.9
d[TpϵA(pT)$_6$]	0.033	0.096	minimum	0.240	0.490	0.503	14.8	16.9
(m = 1)	(±0.003)	(±0.010)	isotropic			0.667	15.5	17.7
			maximum	0.240	0.490	0.993	16.6	19.1
d[(Tp)$_3$ϵA(pT)$_4$]	0.039	0.112	minimum	0.280	0.529	0.490	16.4	19.5
(m = 3)	(±0.003)	(±0.006)	isotropic			0.667	17.3	20.7
			maximum	0.280	0.529	1.019	18.6	22.1
d[(Tp)$_5$ϵA(pT)$_2$]	0.041	0.109	minimum	0.273	0.522	0.492	16.4	19.5
(m = 5)	(±0.004)	(±0.003)	isotropic			0.667	17.2	20.5
			maximum	0.273	0.522	1.015	18.4	21.9
d[(Tp)$_6$ϵApT]	0.031	0.109	minimum	0.273	0.522	0.492	15.4	18.0
(m = 6)	(±0.004)	(±0.003)	isotropic			0.667	16.2	19.0
			maximum	0.273	0.522	1.015	17.4	20.4
d[(pT)$_7$ϵA]	0.020	0.080	minimum	0.200	0.447	0.518	16.8	17.8
(m = 7)	(±0.003)	(±0.002)	isotropic			0.667	17.5	18.6
			maximum	0.200	0.447	0.964	18.6	19.8

[a] λ_{ex} = 320 nm (2-nm band-pass), 25 °C. See Materials and Methods for other details. [b] Calculated by using the mean value of $r_{complex}$ in each case. [c] The value in parentheses is the standard error based on 2–4 independent determinations.

turn relate to the maximum and minimum values of R_0 and thus R (eqs 11–12), also summarized in Table IV.

Discussion

In this paper, we demonstrate that a single ϵA-oligonucleotide of length l = 6–8 binds to the g32P-(A+B) core fragment with a singular polarity of the phosphodiester backbone. Individual nucleotide bases within an l = 8 ϵA-oligonucleotide would therefore be expected to experience structurally distinct regions of the ssDNA-binding site *at or near nucleotide resolution*. We show that fluorescence resonance energy transfer (FRET) spectroscopy can be used to estimate the two-dimensional distance between the intrinsic (fixed) metal ion [Co(II)] of g32P-(A+B) and a uniquely positioned fluorescent ϵ-adenine, functioning as fluorescence energy acceptor and donor, respectively. The same donor–acceptor distance can then be measured in a series of uniquely fluorescently labeled protein–oligonucleotide complexes obtained by variably positioning the ϵA moiety in the primary structure of the bound oligonucleotide. A set of such distances superimposed on a single protein–oligonucleotide complex can then be used to place limitations on the conformation of the bound ssDNA, in addition to providing a rich source of information on local structural features of the g32P core fragment–octanucleotide complex.

The chemistry employed to make 1,N^6-ethenoadenylated oligonucleotides (Figure 1) is identical with published accounts that effect specific modificaton of the adenine, adenosine mononucleotides (Secrist et al., 1972), and adenosine-containing dinucleotides (Tolman et al., 1974; Leonard, 1984). This report provides the first account of modification and subsequent purification of oligonucleotides longer than trimers (Barrio et al., 1978). The purification scheme (Figure 2) is particularly noteworthy since even small amounts of contaminating ϵA monomer will render meaningless determinations of both fluorescence properties due to its ≈12–18-fold greater quantum yield relative to the ϵA-oligonucleotides (Table I).

It is known that the binding of g32P to polynucleotides and natural ssDNAs increases the local base–base separation; similar deformations in oligonucleotide structure have also been shown to occur [cf. Karpel (1990)]. This would result in an enhanced quantum efficiency of the ϵA-base, since intra- (Tolman et al., 1974) and intermolecular (Kubota et al., 1979) nucleotide base stacking strongly quenches ϵA fluorescence through both static (ground-state) and dynamic (excited-state) processes. We use this property of ϵA-oligonucleotides to establish that these ssDNA molecules bind to the g32P-(A+B) core fragment with a defined polarity of the phosphodiester backbone. This is evident in that two pairs of ϵA-oligonucleotides of inverted polarities bind to the core fragment with similar or identical affinities, but Q_d, the quantum yields, and $r_{complex}$, the anisotropies, of the ϵA-oligonucleotide–protein complex are significantly different from one another (Figure 4; Table IV). If both polarities of the phosphodiester backbone were equally acceptable to the core fragment, the fluorescence properties of two symmetric ssDNAs in the complex would be indistinguishable. This is therefore a direct indication that the immediate microenvironments of the ϵA-base are easily distinguishable at the 5′ and 3′ ends of the nucleic acid binding site on the core fragment.

Previous studies have shown that the indole fluorescence emission can be quenched by the ϵA-base via a Trp → ϵA energy transfer process (Mutai et al., 1975). In particular, the complex formed between *uniformly* labeled poly(ϵA) and g32P suggested that at least one tryptophan in g32P is able to transfer energy to one or more ϵA-bases (Toulme & Helene, 1980). We provide evidence that at least one Trp side chain specifically lies in the binding site near the 3′ end of bound oligonucleotide, since when complex formation with the l = 8 ϵA-oligonucleotides is monitored at the protein fluorescence emission (Figure 5; Table II), the magnitude of the *quenching* of the total g32P tryptophan fluorescence is significantly *greater* with the probe positioned toward or at the 3′ end of the oligonucleotide. The transfer efficiency and thus proximity, estimated from the $Q_{max,\epsilon A}/Q_{max,A}$ ratio (Table II), peaks at nucleotide residue 7. It has also been observed that in the model compound 1,N^6-etheno-9-[3-(indol-3-yl)propyl]adenine the indole ring will strongly quench the 1,N^6-ethenoadenosine fluorescence upon selective excitation of the ϵA moiety (Gruber & Leonard, 1975). We observe a clear reduction in the quantum efficiency (Q_d) of the d[(Tp)$_6$ϵApT] (ϵA residue 7) complex relative to the d[(Tp)$_5$ϵA(pT)$_2$] and d[(Tp)$_7$ϵA] complexes (Table I).

The proposal that at least one Trp is present at or near the 3′ end of the oligonucleotide binding site is also consistent with the finding that 1,N^6-ethenoadenosine, relative to adenosine, gradually if only slightly (≤2-fold) *enhances* the binding affinity of an oligonucleotide as the unique base is moved toward the 3′ terminus. In contrast, the ϵA and A nucleotides give identical K_{obs} when the unique base is positioned as in m = 0 and m = 1 oligonucleotides or the 5′ terminus (Table II). Since the ϵA moiety is characterized by increased van der Waals dispersion forces than the purine ring at neutral pH and stacks to a greater degree with the indole ring in model compounds (Gruber & Leonard, 1975; Leonard, 1984), the ϵA aromatic ring might be expected to enhance such interactions and thus increase the K_{obs} in a region of the complex where they are predicted to occur.

Site-Specific Dynamics of g32P-(A+B)–Oligonucleotide Complexes. One model of the complex of g32P with single-stranded nucleic acids predicts the presence of series of consecutive "base-binding pockets" that line the ssDNA-binding groove on g32P (Coleman et al., 1986), interactions supplemented by a considerable electrostatic component to the binding free energy (Kowalczykowski et al., 1981; Alma et al., 1983). Each pocket is thought to contain hydrophobic and/or aromatic amino acid side chains positioned in such a manner that one or more might undergo complete or partial intercalation with the nucleic acid bases (Coleman et al., 1986). ^{1}H NMR studies suggest that these aromatic side chains, however, are not rigidly held as a true intercalator would be (Prigodich et al., 1986; Pan et al., 1989b). A refinement of the base-binding pocket model has been proposed on the basis of two-dimensional NMR studies of the complex between the nonreplicative fd gene 5 protein and single-stranded oligo- and polynucleotides (King & Coleman, 1988). In this "dynamic clamp" model, one or at most two nucleotide bases toward the 3′ or 5′ end of the monomer-binding site are engaged in extensive interactions with hydrophobic amino acid side chains, relative to the other three bases, which together constitute the monomer binding site size (King & Coleman, 1988; Kao et al., 1985).

The steady-state anisotropies of the individual ϵA-oligonucleotide–g32P core fragment complexes ($r_{complex}$) do not support a model in which one or a few bases become strongly immobilized at the physical point of a clamp, since a relatively strongly polarized ϵA fluorescence emission is not encountered in any complex. $r_{complex}$ for the m = 3, 5, and 6 complexes are identical within experimental error. The m = 1 complex formed with d[TpϵA(pT)$_6$] is only slightly lower, perhaps related to the uniquely reduced binding affinity of this par-

ticular oligonucleotide sequence (Table II). This similarity among $r_{complex}$ occurs in spite of the fact that r_{free} for individual oligonucleotides decreases monotonically from the internal ϵA-bases to those positioned incrementally closer to *both* oligonucleotide termini. The 5′-terminal ϵA moiety in d[ϵA-$(pT)_7$]-g32P-(A+B) complex exhibits the greatest rotational mobility ($r_{complex}$ = 0.054). This is not, however, due simply to its terminal nature since the 3′-terminal ϵA-base in d-[$(Tp)_7\epsilon$A] has fluorescence properties more like those of an internal base ($r_{complex}$ = 0.080; Q_d = 0.127). These anisotropy data are in qualitative agreement with preliminary EPR studies of site-specific nitroxide spin-labeled oligonucleotides complexed to the core fragment.[6] We emphasize that $r_{complex} > r_{free}$ for all bound ϵA-oligonucleotides, while preliminary anisotropy measurements with the l = 6 and cooperative l = 16 ϵA-oligonucleotide complexes reveal that $r_{complex}$ varies with the approximate molecular size of the complex. This suggests that, in every case, the ϵA moiety is reorienting in a manner at least partly described by macromolecular tumbling of the complex.

Use of FRET To Extract Structural Information on g32P-(A+B)-Oligonucleotide Complexes. We have determined the efficiency of energy transfer between a transition metal cation and the ϵA-base by monitoring the quenching of the steady-state ϵA fluorescence by the metal cation. We and others have ascribed this quencing by a transition metal to a Förster (1959) energy transfer mechanism (Latt et al., 1970; Horrocks et al., 1975; Chatterji et al., 1986; Wu & Tyagi, 1987). Of course, to document an excited-state energy transfer process, the efficiency determined from comparison of the quantum yields and fluorescence lifetimes measured in the presence and absence of energy acceptor must be identical, i.e., $E = 1 - (Q_{da}/Q_d) = 1 - (\tau_{da}/\tau_d)$ (Lakowicz, 1983). In at least two instances with the ϵA-Co(II) donor–acceptor pair, lifetime measurements have yielded transfer efficiency determinations comparable to that obtained with normalized fluorescence intensities (Villafranca et al., 1979; Vanderkoot et al., 1979). Since the extent of ϵA fluorescence quenching by Co(II) in any context requires complex formation and does not vary in a trivial fashion with the Co(II) concentration, we expect that our steady-state measurements are reporting on a process closely adhering to Förster (1959) theory.

In addition, while the anisotropy values obtained for the complexed oligonucleotides ($r_{complex}$) are indicative of modest axial depolarization of the donor that increases the uncertainty in R_o, and thus R, determined for any one donor–acceptor pair, they are not so large as to invalidate the determinations of R for the individual oligonucleotides (Table IV). In fact, with all ϵA-oligonucleotides, excepting the 5′ terminally labeled d[ϵA$(pT)_7$], $r_{complex}$ are quite similar to one another, evidence that there is essentially no uncertainty that originates from imprecise knowledge of κ^2 in the *relative* determinations of R obtained for individual complexes.

Conformation of the Bound Single-Stranded Oligonucleotide. The determination of six metal ion to nucleotide base distances when applied to a single g32P-(A+B)–octanucleotide complex places constraint on the conformation of the bound ssDNA ligand. The trend in the determined spatial separations between the fixed metal ion and a unique ϵA-base clearly reveals that the nucleotide base at *both* the 5′ and 3′ ends makes a relatively closer approach to the metal ion, with the 5′ base (16.0 Å) closest to the metal ion. As the ϵA-base is gradually moved into the interior of the oligonucleotide from both termini, the ϵA moiety becomes *more distant* from the metal ion. For example, the penultimate 5′ (m = 1) and 3′ (m = 6) bases are 17.7 and 19.0 Å from the metal ion, while the ϵA moiety is farthest away in the m = 3 and m = 5 oligonucleotides at ≈20.6 Å from the metal ion.

Although six intermolecular distances to a single fixed point on the protein obviously cannot uniquely define the structure of the bound ssDNA, it is interesting to note that the relative disposition of successive nucleotide bases in the bound oligonucleotide required by the Co(II)–ϵA distances is in qualitative agreement with a recently proposed family of structural models for the polynucleotide conformation in the cooperative g32P–polynucleotide complex (van Amerongen et al., 1990). The bound polynucleotide is modeled to be a right-handed single-stranded helix, markedly underwound and extended relative to a single-strand of B-form dimensions, such that there are approximately 20–24 bases per helical turn corresponding to a small (16 ± 5°) rotation angle per successive base. The predicted base–base distance is ≈5.5 Å, giving rise to a separation of ≈35 Å between the 5′- and 3′-terminal nucleotide bases in an l = 8 oligonucleotide. The ssDNA is proposed to be wrapped around the protein with the protein on the inside of the single-stranded helix. One g32P monomer (assuming n = 8) would cover approximately 40% or one-third to one-half of a single helical turn, corresponding to 120-180° total base rotation between the 5′ and 3′ terminal bases of a bound l = 8 oligonucleotide.

The individual metal ion to nucleotide distances determined in this study are consistent with a bound ssDNA strand that undergoes only moderate rotation per base, as the calculated models implicate. They also require that the fixed Co(II) ion be positioned on the *inside* of the helix in this model, not quite midway between the 5′ and 3′ termini of an l = 8 oligonucleotide but on or near the line that connects these two points. This is consistent with the predicted position of the core fragment itself. Most importantly, in this structure family, nucleotide residue 5 would mark about one-quarter helical turn, so its attached base would be farthest removed from the inside of the helix, and thus the protein itself. Nucleotide bases on the 5′ and 3′ sides of the residue 5 would then make an incrementally closer approach to the inside of the helix (i.e., the metal ion) from the N^6 and N^3 sides of the tricyclic ring, respectively. This is in agreement with the observed trend in Co(II)–ϵA distances. On the other hand, a single-strand of typical B-form or A-form dimensions are both incompatible with the measured distances (data not shown).

Intrinsic Metal Ion–Nucleotide Base Distances in the Context of the Dimensions of the g32P Monomer. These data are the first of any kind that show that the metal ion is physically close enough to the bound ssDNA such that changes in structure and stability which occur upon Zn(II) depletion from g32P can directly alter complex formation. This becomes apparent when one considers the asymmetry of the g32P-(A+B) monomer, characterized by an estimated 5:1 axial ratio (Giedroc et al., 1990). Low-resolution electron microscopy studies on thin crystal lattices of g32P-A[1] (Grant et al., 1991) suggest a prolate ellipsoidal globular structure of the monomer of about 65 × 25 × 25 Å. One of the short axes likely defines the approximate path of the ssDNA across the surface of a g32P-A monomer, since the long axis is simply too long to accommodate a ssDNA molecular of the indicated length [cf. van Amerongen et al. (1990)]. Clearly, the metal ion cannot be on another side of the molecule, far removed from the ssDNA. In fact, if one considers (1) a ≈5-Å shell of structure

[6] D.G. and P. Hopkins, unpublished observations.

that would bury the metal cation, even if a region of the Zn(II) domain is exposed to solvent on the protein surface, and (2) a separation range of ≈6–8 Å between the sugar phosphate backbone and the tip of the exocyclic ϵA ring, this collection of Co(II)–ϵA distances might place the Zn(II) domain within 10 Å or so from an edge(s) of the ssDNA-binding groove, depending primarily on how the individual bases (energy donors) are specifically oriented with respect to the protein surface (the energy acceptor). It becomes easy to appreciate how the Zn(II) domain in g32P could *directly* influence and stabilize common conformational determinants of both protein–protein and protein–nucleic acid interfaces in both the cooperative and noncooperative binding modes, thereby directly contributing to the magnitudes of the intrinsic monomer association constant and the cooperativity parameter (Giedroc et al., 1987; Nadler et al., 1990).

References

Alma, N. C. M., Harmsen, B. J. M., deJong, E. A. M., Ven, J. V. D., & Hilbers, C. W. (1983) *J. Mol. Biol. 163*, 47–63.

Barrio, J. R., Barrio, M. C. G., Leonard, N. J., England, T. E., & Uhlenbeck, O. C. (1978) *Biochemistry 17*, 2077–2081.

Birdsall, B., King, R. W., Wheeler, M. R., Lewis, C. R., Jr., Goode, S. R., Dunlap, R. B., & Roberts, G. C. K. (1983) *Anal. Biochem. 132*, 353.

Brissette, P., Ballou, D. P., & Massey, V. (1989) *Anal. Biochem. 181*, 234–238.

Bujalowski, W., & Lohman, T. M. (1989) *J. Mol. Biol. 207*, 249–268.

Burke, R. L., Alberts, B. M., & Hosoda, J. (1980) *J. Biol. Chem. 255*, 11484–11493.

Casas-Finet, J. R., Toulme, J.-J., Santus, R., & Maki, A. H. (1988) *Eur. J. Biochem. 172*, 641–646.

Chase, J. W., & Williams, K. R. (1986) *Annu. Rev. Biochem. 55*, 103–136.

Chatterji, D., Wu, C.-W., & Wu, F. Y.-H. (1986) *Arch. Biochem. Biophys. 244*, 218–225.

Coleman, J. E., & Giedroc, D. P. (1989) in Metal Ions in Biological Systems (Sigal, H., Ed.) Vol. 25, pp 171–234, Marcel-Dekker, New York.

Coleman, J. E., Williams, K. R., King, G. C., Prigodich, R. V., Shamoo, Y., & Konigsberg, W. H. (1986) *J. Cell. Biochem. 32*, 305–326.

Dale, R. E., Eisenberg, J., & Blumberg, W. E. (1979) *Biophys. J. 26*, 161–193.

Formosa, T., Burke, R. L., & Alberts, B. M. (1983) *Proc. Natl. Acad. Sci. U.S.A. 80*, 2442–2446.

Förster, T. (1959) *Discuss. Faraday Soc. 27*, 7.

Gettins, P., Beecham, J. M., Crews, B. C., & Cunningham, L. W. (1990) *Biochemistry 29*, 7747–7753.

Giedroc, D. P., Keating, K. M., Williams, K. R., Konigsberg, W. H., & Coleman, J. E. (1986) *Proc. Natl. Acad. Sci. U.S.A. 83*, 8452–8456.

Giedroc, D. P., Keating, K. M., Williams, K. R., & Coleman, J. E. (1987) *Biochemistry 26*, 5251–5259.

Giedroc, D. P., Johnson, B. A., Armitage, I. M., & Coleman, J. E. (1989) *Biochemistry 28*, 2410–2418.

Giedroc, D. P., Khan, R., & Barnhart, K. (1990) *J. Biol. Chem. 265*, 11444–11555.

Grant, R. L., Schmid, M. F., & Chiu, W. (1991) *J. Mol. Biol. 217*, 551–562.

Greve, J., Maestre, M. F., Moise, H., & Hosoda, J. (1978) *Biochemistry 17*, 893–898.

Gruber, B. A., & Leonard, N. J. (1975) *Proc. Natl. Acad. Sci. U.S.A. 72*, 3966–3969.

Haas, E., Katzir, E.-K., Steinberg, I. Z. (1978) *Biochemistry 17*, 5064–5070.

Horrocks, W. D., Holmquist, B., & Vallee, B. L. (1975) *Proc. Natl. Acad. Sci. U.S.A. 72*, 4764–4768.

Karpel, R. L. (1990) in *The Biology of Nonspecific DNA–Protein Interactions*, (Revzin, A., Ed.) pp 103–130, CRC Press, Inc., Boca Raton, FL.

Keating, K. M., Ghosaini, L. R., Giedroc, D. P., Williams, K. R., Coleman, J. E., & Sturtevant, J. M. (1988) *Biochemistry 27*, 5240–5245.

King, G. C., & Coleman, J. E. (1988) *Biochemistry 27*, 6947–6953.

Kohwi-Shigematsu, T., Enomoto, T., Yamada, M.-A., Nakanishi, M., Tsuboi, M. (1978) *Proc. Natl. Acad. Sci. U.S.A. 75*, 4689–4693.

Kowalczykowski, S. C., Bear, D. G., & von Hippel, P. H. (1981a) *The Enzymes 14*, 373–444.

Kowalczykowski, S. C., Lonberg, N., Newport, J. W., & von Hippel, P. H. (1981b) *J. Mol. Biol. 145*, 75–104.

Kowalczykowski, S. C., Paul, L. S., Lonberg, N., Newport, J. W., McSwiggen, J. A., & von Hippel, P. H. (1986) *Biochemistry 25*, 1226–1240.

Kubota, Y., Motoda, Y., & Nakamura, H. (1979) *Biophys. Chem. 9*, 105–109.

Lakowicz, J. R. (1983) *Principles in Fluoresence Spectroscopy*, Plenum Press, New York.

Latt, S. A., Auld, D. S., & Vallee, B. L. (1970) *Proc. Natl. Acad. Sci. U.S.A. 67*, 1383–1389.

Ledneva, R. K., Razjivin, A. P., Kost, A. A., & Bogdanov, A. A. (1978) *Nucleic Acids Res. 5*, 4225–4243.

Leonard, N. J. (1984) *CRC Crit. Rev. Biochem. 15*, 125–199.

Moise, H., & Hosoda, J. (1976) *Nature (London) 259*, 455–458.

Mutai, K., Gruber, B. A., & Leonard, N. J. (1975) *J. Am. Chem. Soc. 97*, 4095–4104.

Nadler, S. G., Roberts, W. J., Shamoo, Y., & Williams, K. R. (1990) *J. Biol. Chem. 265*, 10389–10394.

Pan, T., Giedroc, D. P., & Coleman, J. E. (1989a) *Biochemistry 28*, 8828–8832.

Pan, T., King, G. C., & Coleman, J. E. (1989b) *Biochemistry 28*, 8833–8839.

Prigodich, R. V., Casas-Finet, J. R., Williams, K. R., Konigsberg, W. H., & Coleman, J. E. (1984) *Biochemistry 23*, 522–529.

Prigodich, R. V., Shamoo, Y., Williams, K. R., Chase, J. W., Konigsberg, W. H., & Coleman, J. E. (1986) *Biochemistry 25*, 3666–3672.

Secrist, J. A., Barrio, J. R., Leonard, N. J., & Weber, G. (1972) *Biochemistry 11*, 3499–3506.

Shamoo, Y., Ghosaini, L. R., Keating, K. M., Williams, K. R., Sturtevant, J. M., & Konigsberg, W. H. (1989) *Biochemistry 28*, 7409–7417.

Spicer, E. K., Williams, K. R., & Konigsberg, W. H. (1979) *J. Biol. Chem. 254*, 6433–6436.

Tennent, D. L., & McMillin, D. R. (1979) *J. Am. Chem. Soc. 109*, 2307–2311.

Tolman, G. L., Barrio, J. R., & Leonard, N. J. (1974) *Biochemistry 13*, 4869–4878.

Toulme, J. J., & Helene, C. (1980) *Biochim. Biophys. Acta 606*, 95–104.

van Amerongen, H., Kuil, M. E., Scheerhagan, M. A., & van Grondelle, R. (1990) *Biochemistry 29*, 5619–5625.

Vanderkoot, J. M., Weiss, C. J., & Woodrow, G. V. (1979) *Biophys. J. 25*, 263–275.

Villafranca, J. J., Rhee, S. G., & Chock, P. B. (1978) *Proc. Natl. Acad. Sci. U.S.A. 75*, 1255–1259.
Williams, K. R., & Konigsberg, W. H. (1978) *J. Biol. Chem. 253*, 2463–2470.
Williams, K. R., LoPresti, M. B., & Setoguchi, M. (1981) *J. Biol. Chem. 256*, 1754–1762.
Wu, F. Y.-H., & Tyagi, S. C. (1987) *J. Biol. Chem. 262*, 13147–13154.

Stabilities of Consecutive A·C, C·C, G·G, U·C, and U·U Mismatches in RNA Internal Loops: Evidence for Stable Hydrogen-Bonded U·U and C·C+ Pairs†

John SantaLucia, Jr.,‡ Ryszard Kierzek,§ and Douglas H. Turner*,‡
Department of Chemistry, University of Rochester, Rochester, New York 14627, and Institute of Bioorganic Chemistry, Polish Academy of Sciences, 60-704 Poznan, Noskowskiego 12/14, Poland
Received March 12, 1991; Revised Manuscript Received May 24, 1991

ABSTRACT: The stability and structure of RNA duplexes with consecutive A·C, C·A, C·C, G·G, U·C, C·U, and U·U mismatches were studied by UV melting, CD, and NMR. The results are compared to previous results for GA and AA internal loops [SantaLucia, J., Kierzek, R., & Turner, D. H. (1990) *Biochemistry 29*, 8813–8819; Peritz, A., Kierzek, R., & Turner, D. H. (1991) *Biochemistry 30*, 6428–6436)]. The observed order for stability increments of internal loop formation at pH 7 is AG = GA ≈ UU > GG ≥ CA ≥ AA = CU = UC ≥ CC ≥ AC. The results suggest two classes for internal loops with consecutive mismatches: (1) loops that stabilize duplexes and have strong hydrogen bonding and (2) loops that destabilize duplexes and may not have strong hydrogen bonding. Surprisingly, rCGCUUGCG forms a very stable duplex at pH 7 in 1 M NaCl with a T_M of 44.8 °C at 1×10^{-4} M and a $\Delta G°_{37}$ of −7.2 kcal/mol. NOE studies of the imino protons indicate hydrogen bonding within the U·U mismatches in a wobble-type structure. Resonances corresponding to the hydrogen-bonded uridines are located at 11.3 and 10.4 ppm. At neutral pH, rCGCCCGCG is one of the least stable duplexes with a T_M of 33.2 °C and $\Delta G°_{37}$ of −5.1 kcal/mol. Upon lowering the pH to 5.5, however, the T_M increases by 12 °C, and $\Delta G°_{37}$ becomes more favorable by 2.5 kcal/mol. The pH dependence of rCGCCCGCG may be due to protonation of the internal loop C's, since no changes in thermodynamic parameters are observed for rCGCUUGCG between pH 7 and 5.5. Furthermore, two broad imino proton resonances are observed at 10.85 and 10.05 ppm for rCGCCCGCG at pH 5.3, but not at pH 6.5. This is also consistent with C·C+ base pairs forming at pH 5.5. rCGCCAGCG and rGGCACGCC have a small pH dependence, with T_M increases of 5 and 3 °C, respectively, upon lowering the pH from 7 to 5.5. rCGCCUGCG and rCGCUCGCG also show little pH dependence, with T_M increases of 0.8 and 1.4 °C, respectively, upon lowering the pH to 5.5. CD spectra of sequences with CC, CU, UC, and UU internal loops are typical of A-form conformation. CD spectra of AC, CA, and GG have a positive band at 280 nm, similar to that observed for GA and AA internal loops (SantaLucia et al., 1990). CD spectra of all sequences studied, except rCGCCCGCG, are independent of pH. For rCGCCCGCG, a weak negative band at 300 nm is observed at pH 7, but at pH 5.5 a weak positive band is observed. Current algorithms for the prediction of RNA secondary structure assume that the stability of internal loops is not sequence-dependent or depends only on stacking. This study indicates these approximations are wrong. The measured internal loop free energy increments range from −0.6 to +2.3 kcal/mol, and do not correlate with known stacking parameters.

Prediction of RNA structure from sequence has become an increasingly important goal due to the rapid accumulation of nucleic acid sequence information. Applications include identification of consensus structures (Konings & Hogeweg, 1989; Le et al., 1988), understanding of structure–function relationships (de Smit & van Duin, 1990; Yager & von Hippel, 1991; Le et al., 1989), and design of antisense agents (Wickstrom et al., 1988). The most successful methods for prediction of secondary structure have been based on energy minimization using free energy increments for various RNA motifs (Tinoco et al., 1971; Papanicolaou et al., 1984; Turner et al., 1988; Zuker, 1989; Jaeger et al., 1989). The sequence dependence of free energy increments for Watson–Crick base pairs has been determined experimentally (Borer et al., 1974; Freier et al., 1986a). Little is known, however, about the sequence dependence of loop motifs (Gralla & Crothers, 1973a,b; Groebe & Uhlenbeck, 1988; Tuerk et al., 1988; Turner et al., 1988; Varani et al., 1989; SantaLucia et al., 1990).

A common loop motif is the internal loop in which a helix is interrupted by non-Watson–Crick-paired nucleotides on both strands. It has recently been shown that an internal loop containing two consecutive G·A mismatches is more than 2 kcal/mol more stable than one containing two consecutive A·A mismatches (SantaLucia et al., 1990) and that this additional

† This work was supported by National Institutes of Health Grant GM22939 to D.H.T. and by NIH Grant RR 03317 and NSF Grant DBM 8611927 for purchase of the NMR spectrometer. J.S.L. is an E. H. Hooker Fellow.
* Author to whom correspondence should be addressed.
‡ University of Rochester.
§ Polish Academy of Sciences.

0006-2960/91/0430-8242$02.50/0